ELSEVIER

International Journal of Mass Spectrometry 199 (2000) 211–219

International Journal of Mass Spectrometry

Gas-phase reactivity of diastereomeric acetate ion/tributylborate complexes

Antonello Filippi, Maurizio Speranza*

Dipartimento di Studi di Chimica e Tecnologia delle Sostanze Biologicamente Attive, Università di Roma "La Sapienza", 00185 Roma, Italy

Received 1 October 1999; accepted 2 December 1999

Abstract

The reactivity of $(CH_3COOY)_nH^+$ (n = 1, 2) and $(CH_3COOY)CH_3CO^+$ ions [Y = CH_3, C_2H_5, sC_3H_7, (*R*)-sC_4H_9, (*S*)-sC_4H_9, and (*rac*)-sC_4H_9] toward chiral and achiral tributylborates has been measured by Fourier transform ion cyclotron resonance mass spectrometry. Proton transfer between monomeric ions $(CH_3COOY)H^+$ and (*S*,*S*,*S*)-tri-*sec*-butylborate competes with nucleophilic addition of the borate to the CO center of the ion followed by elimination of either a butanol molecule or the mixed borate. A similar reaction network is observed for dimeric ions $(CH_3COOY)_2H^+$, although the presence of a spectator CH_3COOY molecule in the relevant encounter complexes modifies substantially the evolution kinetics as well as the product pattern. Acetyl group transfer from $(CH_3COOY)CH_3CO^+$ to the borate preludes to an intracomplex CH_3COOY-induced elimination reaction. Enantiodifferentiation between (*R*)-$(CH_3COOsBu)H^+$ and (*S*)-$(CH_3COOsBu)H^+$ is achieved by comparing their reactivity towards (*S*,*S*,*S*)-tri-*sec*-butylborate. (Int J Mass Spectrom 199 (2000) 211–219) © 2000 Elsevier Science B.V.

Keywords: Trialkylborates; Chirality; FTICR; Ion/molecule reactions; Kinetics

1. Introduction

Enantiomeric discrimination in living systems normally proceeds through the preliminary aggregation of an enantiomeric pair with a chiral selector to give two diastereomeric molecular complexes of different stability and reactivity. Although traditional methods, such as calorimetry [1], colorimetry [2], and spectroscopy [3], proved very useful in the study of enantioselective intermolecular interactions, increasing attention is nowadays devoted to gas-phase techniques [4], including mass spectrometry [5]. In fact, these techniques allow evaluation of the intrinsic interactions in diastereomeric aggregates by eliminating the leveling effect of the solvent.

Enantiomeric discrimination in mass spectrometry is normally based on the relative stability and fragmentation of diastereomeric ion/molecule complexes, but rarely on their different reaction kinetics. This first preliminary study, carried out by Fourier transform ion cyclotron resonance (FTICR) mass spectrometry, is aimed at ascertaining whether reactivity can be used as a probe for discriminating optically active ions containing a single chiral center. To this purpose, we

* Corresponding author. E-mail: speranza@axrma.uniroma1.it

Dedicated to Professor Henrì Édouard Audier on the occasion of his 60th birthday.

PII S1387-3806(00)00176-7

CH_3COOY		$(CH_3COOY)H^+$ (*m*)	$(CH_3COOY)CH_3CO^+$ (*a*)	$(CH_3COOY)_2H^+$ (*d*)
Y = CH_3	**1**	m_1		
Y = C_2H_5	**2**	m_2		d_2
Y = sC_3H_7	**3**	m_3	a_3	d_3
Y = (*R*)-sC_4H_9	**4**	m_4	a_4	d_4
Y = (*S*)-sC_4H_9	**5**	m_5	a_5	d_5
Y = (*rac*)-sC_4H_9	**6**	m_6	a_6	d_6
Y = (*rac*)-$CH_3CDCH_2CH_3$	$\mathbf{6^D}$	m_6^D	a_6^D	d_6^D

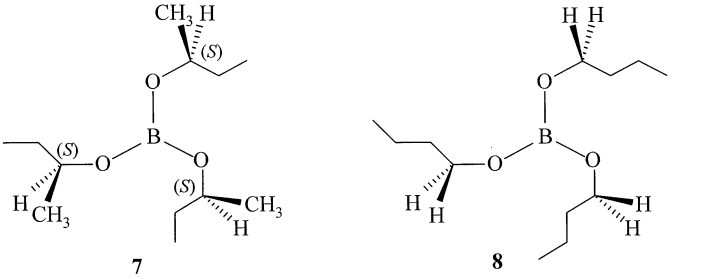

7 **8**

Chart 1.

selected the chiral (*S*,*S*,*S*)-tri-*sec*-butylborate **7** and the achiral tri-*n*-butylborate **8** and measured their reactivity toward a number of acetate ions **m**-**a**-**d**, including those arising from the chiral acetates **4**–**6** (Chart 1). Choice of **7**, as the chiral selector, was determined by its relatively short B–O bond length (1.36 Å) and the cooperative effect of the three *sec*-butyl groups which are expected to magnify the difference in stability and reactivity of the diastereoisomeric adducts between **7** and the chiral acetate ions.

2. Experimental

Acetates **1**–**3** and **6**, as well as tri-*n*-butylborate **8** were purchased from Aldrich Chemical Co. and were purified by preparative gas chromatography (glc) before the use. (*R*)-$CH_3COOsBu$ **4**, (*S*)-$CH_3COOsBu$ **5**, and (*S*,*S*,*S*)-tri-*sec*-butylborate **7** were synthesized from the corresponding chiral 2-butanol (99%, Aldrich Chemical Co.) according to established procedures [6,7]. After careful glc purification, the enantimeric purity of the chiral esters was checked on a Chrompack 9002 gas chromatograph equipped with a flame ionization detector on a 25 m long, 0.25 mm i.d. MEGADEX 5 (30% dimethylpentyl-β-cyclodextrin on OV 1701) fused silica column, operated at temperatures ranging from 40 to 100 °C, 3 °C min^{-1}. The same procedure was used to prepare and purify the racemate of 2-D-2-butyl acetate ($\mathbf{6^D}$) from 2-D-2-butanol. This latter molecule was synthesized by $NaBD_4$ reduction of butanone in anhydrous THF.

The Fourier transform ion cyclotron resonance (FTICR) experiments were carried out at room temperature in a Bruker Spectrospin APEX TM 47e spectrometer equipped with an external ion source and a resonance cell (“infinity cell”) situated between the poles of a superconducting magnet (4.7 T). The external source of the instrument, operating in the chemical ionization (CI) configuration, was fed with the acetates **1**–**6** at nominal pressures ranging around 2×10^{-5} Torr and ionized with 45 eV electrons. Under these conditions, the primary fragments generated in the plasma rapidly react with their neutral precursor to produce high intensities of ions **m**. All of them, but $\mathbf{m_1}$, are accompanied by the corresponding dimers **d** and by the acetylated adducts **a**. The intensity of these species is adequate for a kinetic investigation, except in the case of $\mathbf{a_2}$, which is barely detectable under the experimental condition em-

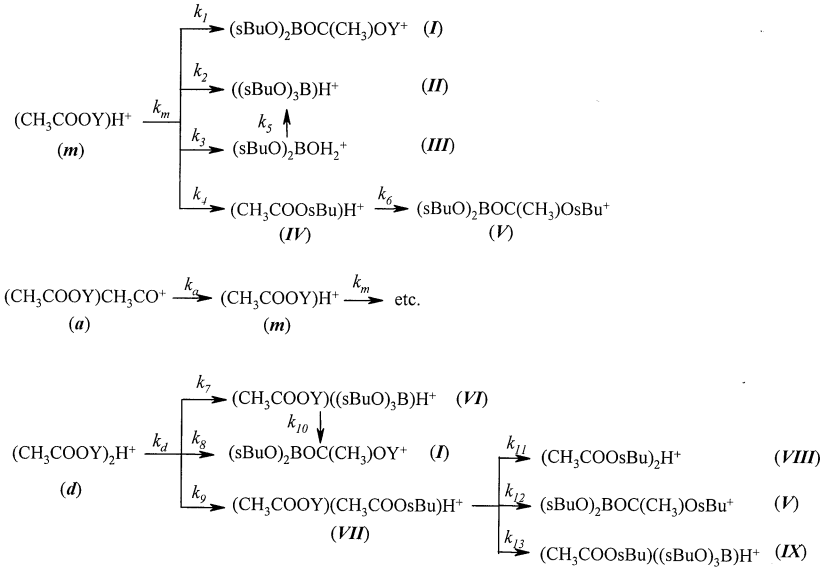

Scheme 1.

ployed. Once formed, the ions were transferred into the resonance cell by a systems of potentials and lenses and quenched by collisions with methane pulsed into the cell through a magnetic valve. The desired ion among **m-a-d** was then isolated from the others by using "single-shots" ejection techniques and allowed to react with borate **7** or **8**, present in the cell at the fixed pressure of 2.6×10^{-8} Torr [8].

3. Results and discussion

The FTICR ion patterns from the attack of ions **m-a-d** on chiral borate **7** are reported in Scheme 1. All steps of Scheme 1 involve a reactive collision between structurally undefined acetate ions with the neutral borate. In all cases, formation of the ionic products is accompanied by release of neutral fragments, which cannot be detected with the experimental method used. Thus, the formulas reported in Scheme 1 are purely indicative of the most probable species and no structural significance should be attached to them.

The reaction networks of Scheme 1 were determined by analysis of the dependence of the corresponding ion abundances on the reaction time. A typical case is illustrated in Fig. 1, concerning the reaction of dimeric ion $\mathbf{d_3}$ with borate **7**. Best fit of the experimental points is represented by the solid lines, which obey the relevant reaction network of Scheme 1 with the following first-order rate constants (in s^{-1}): $k_d = 0.020$; $k_7 = 0.001$; $k_8 = 0.004$; $k_9 = 0.015$; $k_{12} = 0.010$ (neither **VI** $\rightarrow$ **I** conversion (k_{10}), nor formation of **VIII** (k_{11}) and **IX** (k_{13}) from

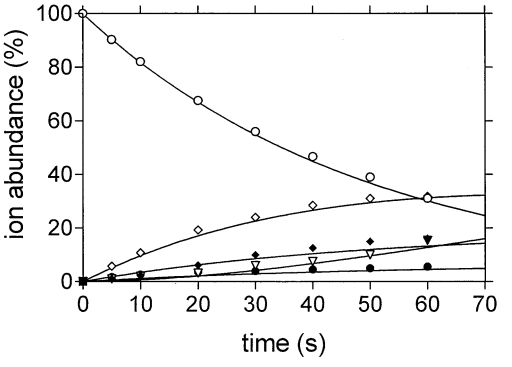

Fig. 1. Time dependence of the relative abundance of the ionic species from attack of $(CH_3COOsC_3H_7)_2H^+$ $\mathbf{d_3}$ (open circles) on (*S*,*S*,*S*)-tri-*sec*-butylborate **7**: **VI** (full circles); **I** (full diamonds); **VII** (open diamonds); **V** (triangles).

Table 1
Phenomenological rate constants ($k_{obs} \times 10^{10}$ cm^3 molecule^{-1} s^{-1}) and efficiencies (eff = k_{obs}/k_{coll}) (in parentheses) of the reactions of ions **m** with tri-*s*-butyl borate **7** (Scheme 1)[a]

Ion	k_m	k_1	k_2	k_3	k_4	k_{coll}	Footnotes
$\mathbf{m_1}$	4.14 (0.30)	...	1.84 (0.13)	2.30 (0.17)	...	13.93	b
$\mathbf{m_2}$	5.58 (0.43)	0.50 (0.04)	2.79 (0.21)	1.68 (0.13)	0.61 (0.05)	13.07	c
$\mathbf{m_3}$	4.48 (0.36)	1.84 (0.15)	1.48 (0.12)	0.85 (0.07)	0.31 (0.02)	12.42	d
$\mathbf{m_4}$	4.89 (0.41)	3.47 (0.29)	1.42 (0.12)	...	...	11.89	
$\mathbf{m_5}$	6.26 (0.52)	3.95 (0.33)	2.31 (0.19)	...	...	11.89	
$\mathbf{m_6}$	5.12 (0.43)	3.81 (0.32)	1.31 (0.11)	...	...	11.89	

[a] The bars denote rate constants below the detection limit of 1×10^{-13} cm^3 molecule^{-1} s^{-1}.
[b] $k_5 = 1.84 \times 10^{10}$ cm^3 molecule^{-1} s^{-1}.
[c] k_n ($\times 10^{10}$ cm^3 molecule^{-1} s^{-1}) = 2.21 (n = 5), 1.39 (n = 6).
[d] k_n ($\times 10^{10}$ cm^3 molecule^{-1} s^{-1}) = 2.21 (n = 5), 0.77 (n = 6).

VII were observed). Further support for the specific reaction sequences of Scheme 1 arises from multiple resonance experiments, involving isolation of the ion of interest, e.g. **VII**, by applying the appropriate frequency window to remove all the undesired ions from the cell and analysis of its progeny, i.e. **V**, after a suitable reaction time.

The first-order rate constants of the individual steps of Scheme 1 were used to derive the corresponding second-order values (k_{obs}), reported in Tables 1–3. The relevant reaction efficiencies (eff) are calculated from the ratio between the experimental k_{obs} and the relevant collision (k_{coll}) rate constant, estimated according to the trajectory calculation method [9].

*3.1. Reactions of $(CH_3COOY)H^+$ ions (**m**) and $(CH_3COOY)CH_3CO^+$ ions (**a**)*

Analysis of Table 1 reveals no direct correlation between the overall reactivity (k_m) of the selected ions **m** toward borate **7** and the nature of the group Y.

Table 2
Phenomenological rate constants ($\times 10^{10}$ cm^3 molecule^{-1} s^{-1}) and efficiencies (eff = k_{obs}/k_{coll}) (in parentheses) of the reactions between ions **a** and tri-*s*-butyl borate **7** (Scheme 1)

Reaction	k_a	k_{coll}
$\mathbf{a_3}$	3.87 (0.35)	11.11
$\mathbf{a_4}$	4.44 (0.41)	10.80
$\mathbf{a_5}$	5.37 (0.50)	10.80
$\mathbf{a_6}$	5.35 (0.49)	10.80

All ions **m** are able to protonate **7** (k_2), although with a limited efficiency. Protonation of **7** may induce partial fragmentation of the relevant intermediate into **III** and a butene molecule (k_3), to an extent which increases with the exothermicity of the process, i.e. in the order $sC_4H_9 < sC_3H_7 < C_2H_5 < CH_3$ [10]. In turn, ions **III** transfer a proton to another molecule of **7** yielding stable **II** (k_5).

Besides protonation, ions **m** react with borate **7** producing **I** (k_1) and **IV** (k_4) with a combined efficiency increasing in the order: $CH_3 < C_2H_5 < sC_3H_7 < sC_4H_9$. Formation of these products requires the addition of the borate to the CO center of **m** yielding the tetrahedral intermediates **X**. These latter may undergo extensive rearrangements followed by the extrusion of either a molecule of butanol [**X** → **XI** → **I**; path (i) of Scheme 2] [11] or the mixed borate $(sBuO)_2BOY$ [**X** → **XII** → **IV**; path (ii) of Scheme 2] [12]. Both processes are clearly detectable with $\mathbf{m_2}$ and $\mathbf{m_3}$, as the reactants.

Of crucial importance for this study it is to check whether path (ii) of Scheme 2 is accessible to protonated *sec*-butyl acetates as well. In fact, the resonant interconversion **X** ⇔ **XII** would lead to extensive scrambling among the *sec*-butoxy groups and, thus, rapid loss of their chiral identity. Verification of this possibility requires the use of labeled $\mathbf{m_6^D}$. The relevant product pattern is characterized by the formation of **I**, retaining the deuterium signature, and of unlabeled **II**. No signs of formation of unlabeled **IV** from $\mathbf{m_6^D}$ have been acknowledged. These findings indicate

Table 3
Phenomenological rate constants ($\times 10^{10}$ cm^3 molecule^{-1} s^{-1}) and efficiencies (eff $= k_{obs}/k_{coll}$) (in parentheses) of the reactions between ions **d** and tri-*s*-butyl borate **7** (Scheme 1)[a]

Ion	k_d	k_7	k_8	k_9	k_{coll}	Footnotes
$\mathbf{d_2}$	0.39 (0.037)	0.09 (0.009)	...	0.3 (0.028)	10.47	b
$\mathbf{d_3}$	0.21 (0.021)	0.01 (0.001)	0.04 (0.004)	0.16 (0.016)	10.06	c
$\mathbf{d_4}$	0.07 (0.007)	0.03 (0.003)	0.04 (0.004)	...	9.73	d
$\mathbf{d_5}$	0.08 (0.008)	0.03 (0.003)	0.05 (0.005)	...	9.73	e
$\mathbf{d_6}$	0.08 (0.008)	0.03 (0.003)	0.05 (0.005)	...	9.73	f

[a] See footnote a of Table 1.
[b] $k_{10} = 0.02$ s^{-1}; k_n ($\times 10^{10}$ cm^3 molecule^{-1} s^{-1}) = 0.10 ($n = 11$), 0.29 ($n = 12$), $n = 0.05$ ($n = 13$).
[c] $k_{10} < 10^{-4}$ s^{-1}; k_{12} ($\times 10^{10}$ cm^3 molecule^{-1} s^{-1}) = 0.06.
[d] $k_{10} = 0.04$ s^{-1}.
[e] $k_{10} = 0.05$ s^{-1}.
[f] $k_{10} = 0.04$ s^{-1}

that path (i) of Scheme 2 (Y = *s*Bu) largely supersedes the competing transesterification (ii) and that, therefore, no scrambling of the chiral *sec*-butoxy moieties takes place in the reaction between chiral $\mathbf{m_4}$–$\mathbf{m_6}$ and **7**. This conclusion lines up with the marked increase of the k_1/k_4 ratio in going from $\mathbf{m_2}$ ($k_1/k_4 = 0.8$) to $\mathbf{m_3}$ ($k_1/k_4 = 5.9$) (Table 1). The same conclusions are reached with tri-*n*-butylborate **8**, as the substrate. In this case, k_n ($\times 10^{-10}$ cm^3 molecule^{-1} s^{-1}) = 0.81 (eff = 0.07) ($n = 1$); 2.4 (eff = 0.20) ($n = 2$); <0.001 ($n = 3$ and 4). Decrease of the efficiency of path (i) of Scheme 2 in passing from **7** to **8** (Table 1) is explanable in terms of the lower migratory aptitude of the *n*-butyl versus the *sec*-butyl group.

Incidentally, it should be noted that path (ii) of Scheme 2 with Y = sC_3H_7 leads to the exclusive formation of **IV**, and not to $(s\mathrm{BuO})_2\mathrm{BO(H)Y}^+$. This observation, coupled with the formation of fair amounts of **II** from $\mathbf{m_6}$ (Table 1), implies necessarily that the PA of *sec*-butyl acetate exceeds that of $(s\mathrm{BuO})_2\mathrm{BO}sC_3H_7$ and is close to that of $(s\mathrm{BuO})_3\mathrm{B}$ [10].

Particularly intriguing is the exclusive formation of **m** (Y = sC_3H_7 and sC_4H_9) from attack of the corresponding ions **a** on borates **7** and **8** (Scheme 1 and Table 2). Indeed, with $\mathbf{a_6^D}$, the reactions lead to the formation of both $\mathbf{m_6}$ and $\mathbf{m_6^D}$, in approximately constant proportions, i.e. $\mathbf{m_6}$ (~70%) and $\mathbf{m_6^D}$ (~30%). This isotopomeric distribution closely matches that expected from complete interchange of the butyl groups in the **a**/borate adduct and is there-

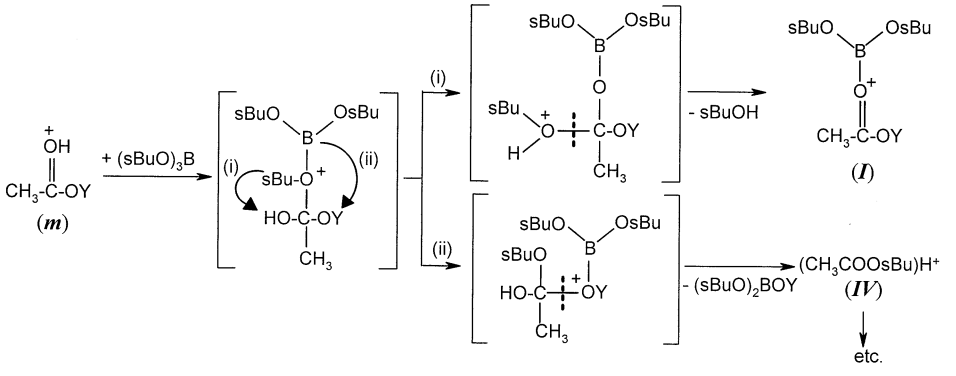

Scheme 2.

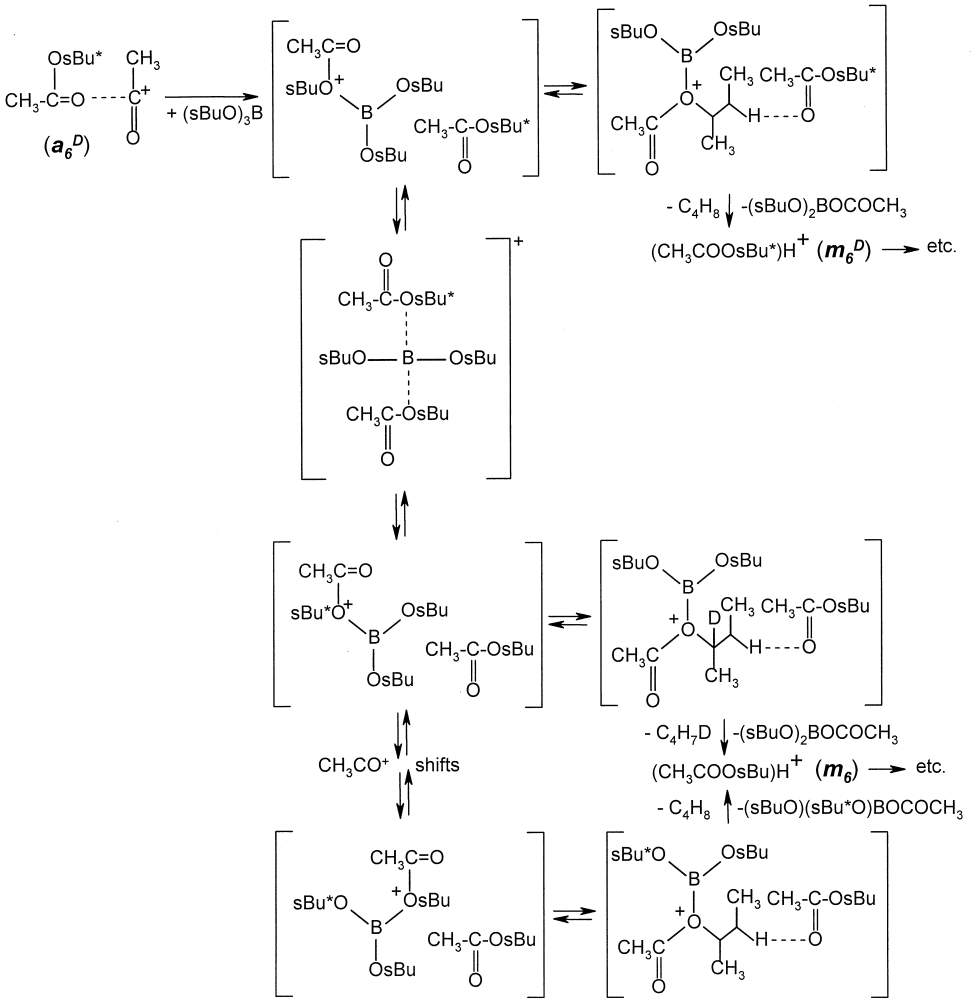

Scheme 3.

fore inconsistent with the simple hypothesis of the collision induced decomposition of **a** to **m** and ketene in the FTICR cell. A plausible rationale of all the experimental evidence is provided by the elimination pattern shown in Scheme 3 (*s*Bu* = $CH_3CDCH_2CH_3$).

3.2. Reactions of $(CH_3COOY)_2H^+$ ions (**d**)

Dimers **d** exhibit an overall reactivity towards borate **7** which is several orders of magnitude lower than that of the corresponding monomers **m** and which increases in the order: $sC_4H_9 < sC_3H_7 < C_2H_5$ (k_d in Table 3).

Although the unfavorable thermochemistry prevents formation of the protonated borate **II** from **d** [13], the observed product pattern is found to parallel that of the corresponding monomers **m**, with the only difference that the corresponding reaction intermediates contain an additional CH_3COOY molecule (Scheme 4). Formal extrusion of a butanol molecule and of the spectator acetate from adducts **XIV** leads to the formation of ion **I** [path (i) of Scheme 4] (k_8 in Table 3), whereas formal loss of a $(sBuO)_2BOY$ molecule from **XV** yields ion **VII** [path (ii) of Scheme 4] (k_9 in Table 3).

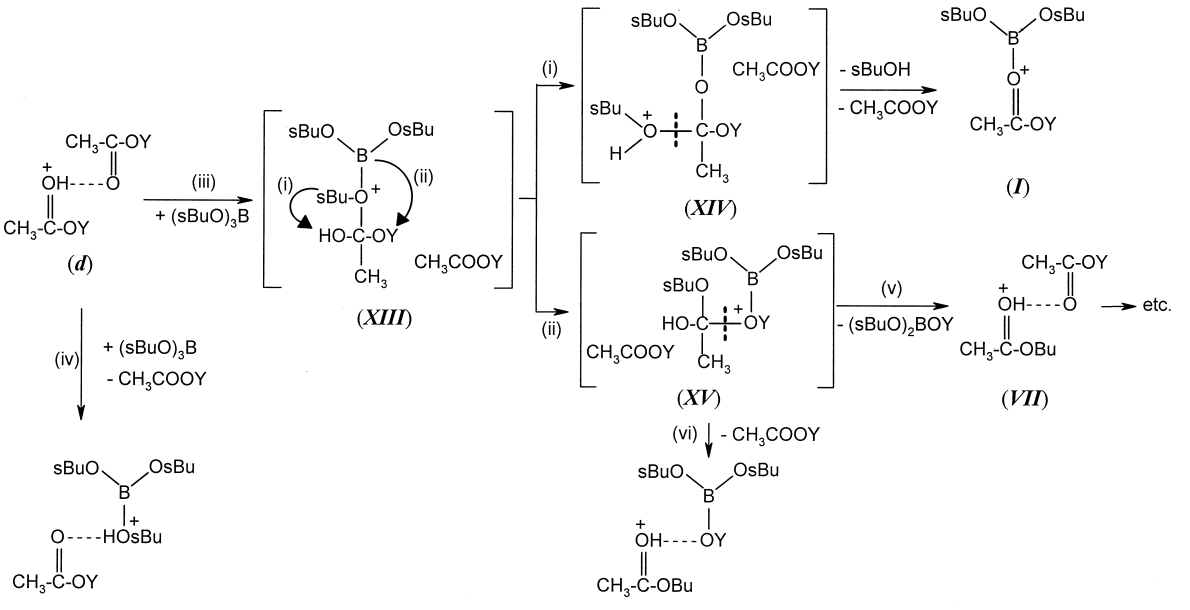

Scheme 4.

Two different mechanisms for the k_7 path leading to **VI** can be considered. One involves elimination of the spectator CH_3COOY molecule from **XV** with formation of the $(CH_3COOsBu)[(sBuO)_2BOY]H^+$ product [path (vi) of Scheme 4]. The other proceeds through a simple $(sBuO)_3B$-to-CH_3COOY ligand displacement in **d**, yielding the $(CH_3COOY)[(sBuO)_3B]H^+$ isobar [path (iv) of Scheme 4]. Clearcut discrimination between these mechanistic hypotheses is inaccessible, except perhaps in the reaction of **7** with $\mathbf{m_6^D}$. In this case, product **VI** from path k_7 is found to contain only one deuterium atom, in agreement with the ligand displacement (iv). No uptake of two deuteriums was observed in the product, as one would expect from **XV** if equally releasing either $CH_3COOsBu$ or CH_3COOY [path (vi); Y = *s*Bu*]. This means that the transesterification path (ii) of Scheme 4 is inhibited to dimers $\mathbf{d_6}$ (and $\mathbf{d_6^D}$), much like it is the corresponding transesterification (ii) of Scheme 2 to monomers $\mathbf{m_6}$ (and $\mathbf{m_6^D}$). This conclusion is reinforced by the complete absence of the monodeuterated ion **VII** among the reaction products from $\mathbf{d_6^D}$ (k_9 in Table 3).

The agreement between the behavior of dimers **d** and that of their monomeric analogs **m** applies also as to the dependence of the (i) versus (ii) branching ratio upon the nature of the Y group. As for **m**, the efficiency of path (i) increases in the order $C_2H_5 < sC_3H_7 < sC_4H_9$ and that of the competing path (ii) increases in the opposite order.

3.3. Chiral systems

The results reported in Table 1 point to some differences in both the overall reactivity of chiral $\mathbf{m_4}$–$\mathbf{m_6}$ toward **7** and the relative extent of the competing addition (k_1) and protonation pathways (k_2) of Scheme 1. Fig. 2 illustrates these differences, observed in all runs and under circumstances excluding any mass effect on ion detection. It clearly indicates that (*S*,*S*,*S*)-tri-*sec*-butylborate **7** reacts more efficiently with the homochiral (*S*)-ion $\mathbf{m_5}$ than with the heterochiral (*R*)-ion $\mathbf{m_4}$. The reaction efficiency of the racemate $\mathbf{m_6}$ falls in between. A similar picture is observed for the acetylated reactants **a** (Table 2), whereas no pronounced reactivity differences are found for dimers **d** (Table 3). Evaluation of the significance of these differences requires a careful

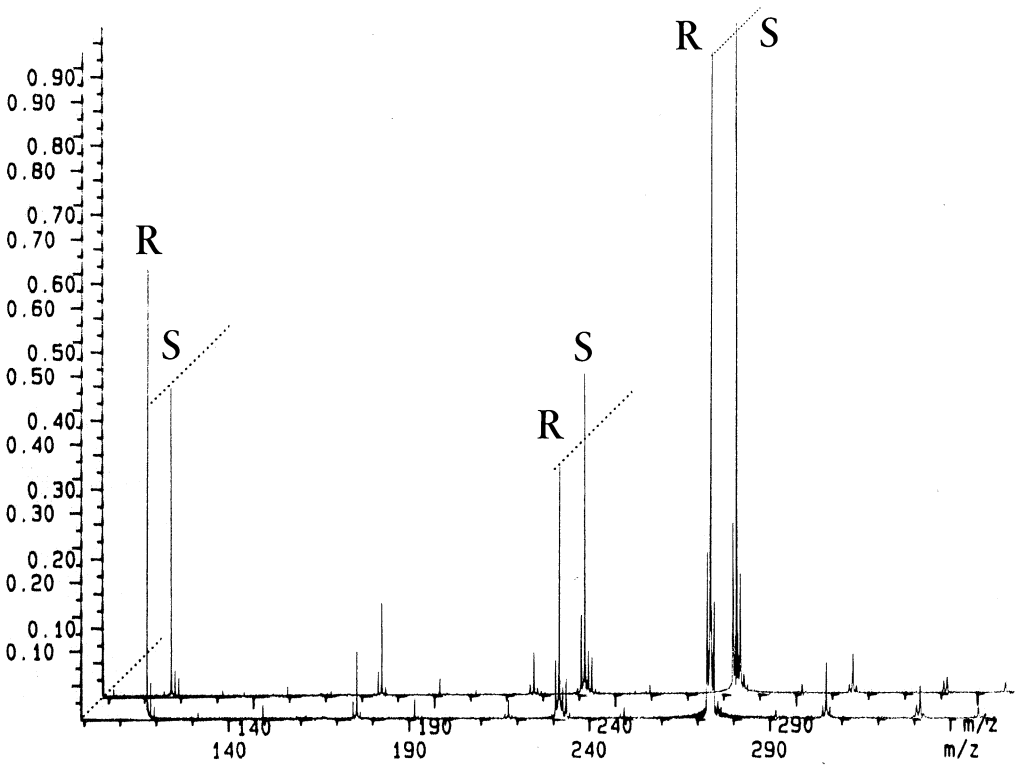

Fig. 2. Comparison of the mass spectra showing the $((s\text{BuO})_3\text{B})\text{H}^+$ (m/z 231) and $(s\text{BuO})_2\text{BOC}(\text{CH}_3)\text{OsBu}^+$ (m/z 273) products obtained from attack of $\mathbf{m_4}$ (**R**) (m/z 117) and $\mathbf{m_5}$ (**S**) (m/z 117) on (*S*,*S*,*S*)-tri-*sec*-butylborate **7** (2.6×10^{-8} torr) after 3 s reaction time.

analysis of the precision of the kinetic results of Tables 1 and 2 and an estimate of the attached uncertainty levels. The high precision of the kinetic measurements is demonstrated by the observation that the reaction efficiency of the homochiral pair, invariably exceeds that of the heterochiral one in all runs. The standard deviation associated to the absolute rate constants of Tables 1 and 2 is estimated as not exceeding 15% and the combined uncertainty attached to their difference is computed as below 20%. In this frame, the overall reactivity (k_m) of the (*R*)-ion $\mathbf{m_4}$ toward **7** cannot be considered as different from that of racemate $\mathbf{m_6}$. Nevertheless, some reactivity difference just beyond the combined standard deviations is observed between the (*R*)-ion $\mathbf{m_4}$ and the (*S*)-ion $\mathbf{m_5}$ (Table 1). No similar conclusions can be derived from the experiments with chiral **a** since the corresponding reactivity differences fall all within the combined uncertainties (Table 2). Reactivity differences between the (*R*)-ion $\mathbf{m_4}$ and the (*S*)-ion $\mathbf{m_5}$ extend also to the relative extent of the competing addition (k_1) and protonation pathways (k_2) of Scheme 1 (Table 1). Thus, the $k_1/k_2 = 2.4$ ratio, measured for the (*R*)-ion $\mathbf{m_4}$, decreases to 1.7 for the (*S*)-ion $\mathbf{m_5}$ (Table 1).

Although the sizable uncertainty of the FTICR kinetic measurements warns us from making of the present results an outstanding example of chiral discrimination gas phase, it also drives us to search for better conditions and more adequate chiral selectors which would make the reactivity approach a reliable tool for this important task.

Acknowledgements

Work supported by the Ministero dell'Università e della Ricerca Scientifica e Tecnologica (MURST) and

the Consiglio Nazionale delle Ricerche (CNR). The authors express their gratitude to Fausto Angelelli for his technical assistance.

References

[1] E.M. Arnett, S.P. Zingg, J. Am. Chem. Soc. 103 (1981) 1221.
[2] Y. Kubo, S. Maeda, S. Tokita, M. Kubo, Nature 382 (1996) 522.
[3] D. Parker, Chem. Rev. 91 (1991) 1441.
[4] A. Latini, D. Toja, A. Giardini Guidoni, A. Palleschi, S. Piccirillo, M. Speranza, Chirality 11 (1999) 376, and references therein.
[5] (a) M. Sawada, Mass Spectrom. Rev. 16 (1995) 73, and references therein; (b) W. Shen, P.S.H. Wong, R.G. Cooks, Rapid Commun. Mass Spectrom. 11 (1997) 71; (c) J. Ramirez, F. He, C. Lebrilla, J. Am. Chem. Soc. 120 (1998) 7387.
[6] G. Höfle, W. Steglich, H. Vorbrüggen, Angew. Chem. Int. Ed. Engl. 17 (1978) 569.
[7] C.A. Brown, S. Krishnamurthy, J. Org. Chem. 43 (1978) 2731.
[8] The actual pressure of borates in the FTICR cell was estimated by correcting the ionization gauge reading according to the procedure proposed in: J.E. Bartmess, R.M. Georgiadis, Vacuum 33 (1983) 149.
[9] T. Su, W.J. Chesnavich, J. Chem. Phys. 76 (1982) 5183.
[10] PA(CH_3COOY) (kcal mol^{-1}) = 196.4 (Y = CH_3); 199.7 (Y = C_2H_5); 199.9 (Y = sC_3H_7). As for alkanol, the PA of acetates is expected to reach a limit which can be place several kilocalories per mol above that of $CH_3COOsC_3H_7$ [S.G. Lias, J.E. Bartmess, J.F. Liebman, J.L. Holmes, R.D. Levin, W.G. Mallard, J. Phys. Chem. Ref. Data 17 (1988) Suppl. No. 1]. Taking into account that the PA at the ethoxy group of $(CH_3O)_2BOC_2H_5$ is 201 kcal mol^{-1} [11], the PA of **7** and **8** is expected to slightly exceed this value (see text). Accordingly, the exothermicity of the protonation of the selected borates with $(CH_3COOY)H^+$ decreases with the Y order: $CH_3 > C_2H_5 > sC_3H_7 > sC_4H_9$.
[11] T.D. Ranatunga, H.I. Kenttämaa, Inorg. Chem. 34 (1995) 18.
[12] Another conceivable route to product **I** involves preliminary proton transfer from **m** to **7**, followed by nucleophilic displacement of the so formed neutral acetate at the boron center with extrusion of the butanol molecule. Work is in progress to check this possibility.
[13] The association energy of an oxygen-containing molecule with its protonated derivative may amount to several tens of kilocalories per mole (see, for instance: P. Kebarle, Ions and Ion Pairs in Organic Reactions, M. Szwarc (Ed.), Wiley, New York, 1972, Chap. 2; P. Kebarle Ion Molecule Reactions, J.L. Franklin (Ed.), Plenum, New York, 1972, Chap. 7). Thus, the PA of the dimeric forms may exceed that of the bare molecule by the same quantity.